Phonon-Terminated Optical Masers

L. F. JOHNSON, H. J. GUGGENHEIM, AND R. A. THOMAS
Bell Telephone Laboratories, Murray Hill, New Jersey
(Received 11 April 1966)

The characteristics of phonon-terminated coherent oscillation associated with Ni^{2+}, Co^{2+}, and V^{2+} ions in rutile and perovskite fluorides are described. Continuous tunability over portions of the vibronic continuum of Ni^{2+} in MgF_2 has been demonstrated. The system has been thermally tuned in discontinuous segments over a total wavelength span from 1.62 to 1.80 μ, the longest continuous segment being 250 Å (82 cm^{-1}). Alternatively, a frequency-selective element (prism) has been used to vary the oscillation frequency (at a fixed temperature of 85°K) in discontinuous segments between 1.62 and 1.84 μ. The discontinuities are a consequence of structure present in the vibronic continuum of Ni^{2+} in MgF_2. Continuous-wave oscillation has been obtained from Ni^{2+} ions in MgF_2 and MnF_2, requiring, respectively, less than 65 and 240 W of power into a tungsten lamp. Both systems display continuous spiking, and the spectral distributions of maser emission may be very complex.

1. INTRODUCTION

THE fluorescence spectra of transition metal ions in crystals are usually characterized by sharp electronic (no-phonon) lines accompanied by broad vibronic sidebands corresponding to electronic transitions with simultaneous vibrational excitation of the lattice (phonon emission). The coherent emission associated with Ni^{2+}, Co^{2+}, and V^{2+} ions in rutile and perovskite fluorides is unusual in that the preferred region for maser oscillation lies in the vibronic continuum, i.e., the terminal state of the maser transition represents an excited vibrational state of the lattice-impurity system.[1,2] Using a phenomenological approach, McCumber has developed a theory for phonon-terminated optical masers[3,4] which suggests the possibility of constructing oscillators which are tunable over a broad range. We have demonstrated continuous tunability over portions of the vibronic continuum of Ni^{2+} in MgF_2. The system has been thermally tuned in discontinuous segments over a total wavelength span from 1.62 to 1.8 μ, the longest continuous segment being 250 Å (82 cm^{-1}). Alternatively, a frequency-selective element (prism) has been used to vary the oscillation frequency (at a fixed temperature of 85°K) in discontinuous segments between 1.62 and 1.84 μ. The discontinuities are a consequence of structure present in the vibronic continuum of Ni^{2+} in MgF_2. Continuous-wave (CW) oscillation has been obtained from Ni^{2+} ions in MgF_2 and MnF_2 requiring, respectively, less than 65 and 240 W of power into a tungsten lamp. Both systems display continuous spiking, and the spectral distributions of maser emission may be very complex. The combination of low threshold and tunability should make it possible to construct a tunable source of continuous coherent emission.

[1] L. F. Johnson, R. E. Dietz, and H. J. Guggenheim, Phys. Rev. Letters **11**, 318 (1963).
[2] L. F. Johnson, R. E. Dietz, and H. J. Guggenheim, Appl. Phys. Letters **5**, 21 (1964).
[3] D. E. McCumber, Phys. Rev. **134**, A299 (1964).
[4] D. E. McCumber, Phys. Rev. **136**, A954 (1964).

2. EXPERIMENTAL

Spontaneous and stimulated emission spectra were recorded with a Perkin-Elmer model 112G grating spectrometer in conjunction with PbS and cooled gold-doped germanium detectors. Thermal tuning of coherent emission was obtained under pulse illumination in an FT-524 helical xenon lamp. Crystal temperature was controlled by cooled nitrogen gas and monitored by a copper-constantan thermocouple. CW oscillation was produced in a cylindrical-ellipse pumping configuration, with the crystal at one focus and a 500-W T3Q iodine quartz tungsten lamp at the other. The crystal was cooled to 85°K by liquid oxygen pre-cooled by liquid nitrogen to eliminate bubbling.

3. THERMAL TUNING OF MgF_2:Ni^{2+}

The π-polarized absorption spectrum (E vector parallel to c-axis) of Ni^{2+} in MgF_2 at 20°K is shown in Fig. 1. The absorption coefficient is plotted horizontally and the bands are labeled with reference to the theory of Tanabe and Sugano.[5] Fluorescence is produced in transitions between the first excited state $^3T_2$ and the ground state $^3A_2$. Emission spectra at 20°K are shown in Fig. 2. The strong lines near 1.54 μ identify pure electronic transitions of the Ni^{2+} ion, while the broad sideband is vibronic. The maser frequency coincides with the frequency of maximum emission on the vibronic continuum. π-polarized emission spectra at higher temperatures are shown in Fig. 3, where it will be noted that the maser frequency shifts to longer wavelength with increasing temperature. A striking feature is that, at these temperatures, oscillation is not observed at 1.62 μ, the frequency of maximum emission on the vibronic sideband. A complete description of the thermal tuning of coherent emission in MgF_2:Ni^{2+} (1.5%) is presented in Fig. 4. Between 20 and 240°K the wavelength varies over five discontinuous segments between 1.62 and 1.8 μ, the longest continuous segment

[5] Y. Tanabe and S. Sugano, J. Phys. Soc. (Japan) **9**, 753, 766 (1954).

being a 250-Å span between 1.731 and 1.756 μ (82 cm^{-1}). The oscillation threshold increases from 140 to 1700 J over this temperature range. The discontinuities are a consequence of structure present in the vibronic continuum. This structure is evident in the emission spectra of Fig. 3, in which the temperatures were chosen to correspond to points on four different segments of the thermal-tuning data in Fig. 4. A comparison of Figs. 3 and 4 reveals that with increasing temperature, oscillation shifts from frequencies in the neighborhood of one vibronic peak to another.

To provide a quantitative description of thermal-tuning phenomena, we apply McCumber's theory for phonon-terminated optical masers. Basic to this description is McCumber's expression for $g(\mathbf{k},\omega)$, the gain per unit length for radiation of frequency ω and wave vector parallel to the unit vector $\mathbf{k}$:

$$g_\pi(\mathbf{k},\omega)=\{N_+-N_-\exp[\hbar(\omega-\omega_0)/kT]\sigma_{e\pi}(\mathbf{k},\omega)\}, \quad (1)$$

where N_+ and N_- are the total populations per unit volume of the upper and lower states (electronic plus vibrational levels), respectively; $\hbar(\omega-\omega_0)$ = energy measured from the no-phonon line[6] at $\hbar\omega_0$ = 6500 cm^{-1}. The cross section for stimulated emission $\sigma_{e\pi}(\mathbf{k},\omega)$ is obtained from the fluorescence spectrum according to

$$\sigma_{e\pi}=f_\pi(\mathbf{k},\omega)\left[\frac{2\pi c}{\omega n_\pi(\mathbf{k},\omega)}\right]^2, \quad (2)$$

where $f_\pi(\mathbf{k},\omega)d\Omega$ is the fluorescence intensity in photons/sec *per unit frequency interval* of π-polarized radiation

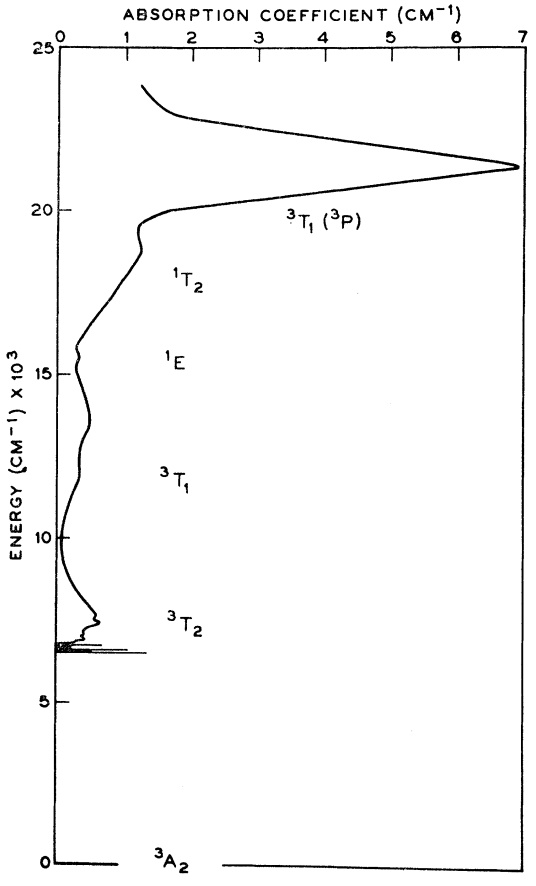

FIG. 1. The π-polarized absorption spectrum of MgF_2:Ni^{2+} (0.5%) at 20°K. The absorption coefficient is given by the horizontal scale at the top. Fluorescence is produced in transitions between the first excited state $^3T_2$ and the ground state $^3A_2$.

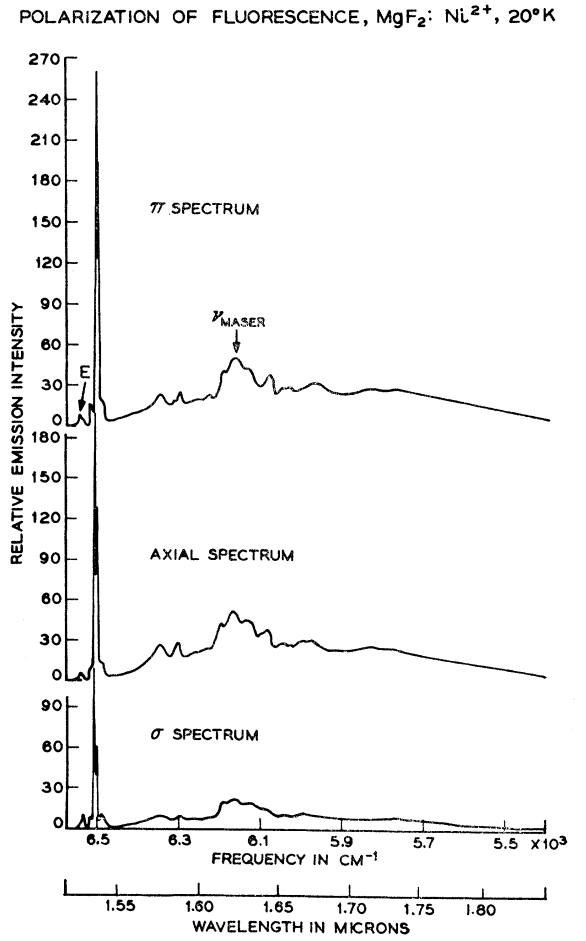

FIG. 2. Polarization of the $^3T_2 \rightarrow {}^3A_2$ emission of MgF_2:Ni^{2+} (1%) at 20°K (taken from Ref. 1). The intense narrow lines near 1.54 μ correspond to pure electronic transitions of the Ni^{2+} ion, while the broad sideband is vibronic (electronic transitions with simultaneous vibrational excitation of the lattice). The maser frequency is indicated by the arrow.

of frequency ω emitted into solid angle $d\Omega$ by each excited fluorescing ion; $n_\pi(\mathbf{k},\omega)$ is the index of refraction. We restrict our analysis to emission with π

[6] Strictly speaking, the ground state of Ni^{2+} in MgF_2 is split into three components so that the "no-phonon line" actually consists of a triplet with an over-all splitting of 6 cm^{-1}. We ignore this splitting since it is small in comparison to the energy differences with which we are concerned. Furthermore, additional no-phonon lines appear with increasing temperature at energies higher than $\hbar\omega_0$, but these are weak and are likewise neglected.

polarization since it is stronger than σ by about a factor of 3. In any event, the vibronic π and σ spectra are quite similar in spectral detail.

Briefly, the gain expression represents the difference between a stimulated-emission coefficient $e_\pi = N_+\sigma_{e\pi}$ and an absorption coefficient

$$\alpha_\pi = N_- \exp[\hbar(\omega-\omega_0)/kT]\sigma_{e\pi}.$$

A remarkable result of McCumber's analysis is that *both* the emission *and* absorption terms may be inferred from the fluorescence spectrum alone. The absorption term represents the thermal population of the vibrational density of states associated with the ground electronic state. At $T=0$, absorption in the vibronic sideband ($\omega-\omega_0<0$) is zero and the gain is proportional to the fluorescence intensity f times ν^{-2}. Oscillation occurs at the frequency of maximum $f\nu^{-2}$. At

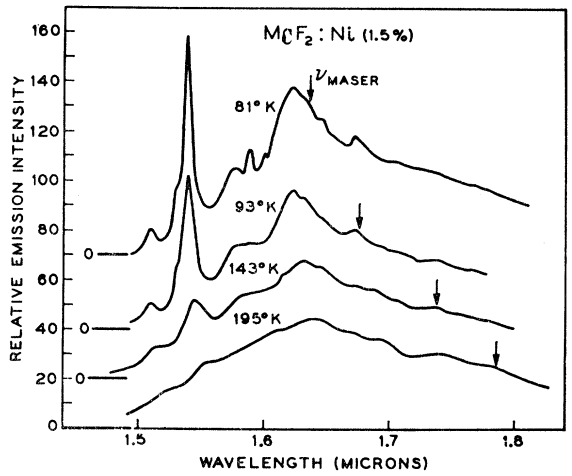

FIG. 3. π-polarized emission spectra of $MgF_2:Ni^{2+}$ (1.5%) at 81, 93, 143, and 195°K. The maser frequency at each temperature is indicated by an arrow. Spectra are recorded at constant *wavelength* interval.

finite temperatures, the importance of the absorption term depends on the relative magnitude of N_+ and $N_- \exp[\hbar(\omega-\omega_0)/kT]$. We are particularly concerned here with situations in which reflection and internal scattering losses are small. Then the threshold excited-state population N_+ is also small and the absorption and stimulated emission terms may be comparable over much of the vibronic sideband. The effect on the gain spectrum is that as the upper state threshold population N_+ decreases, the gain maximum shifts to progressively lower frequencies. Correspondingly, increasing the temperature causes a similar shift in the gain spectrum. This is demonstrated by the gain curves of Fig. 5, calculated from the emission spectra of Fig. 3. The threshold population N_+ at 81°K was computed by combining the absorption spectrum, integrated over the spectral distribution of the pump lamp, with measured values of lifetime, quan-

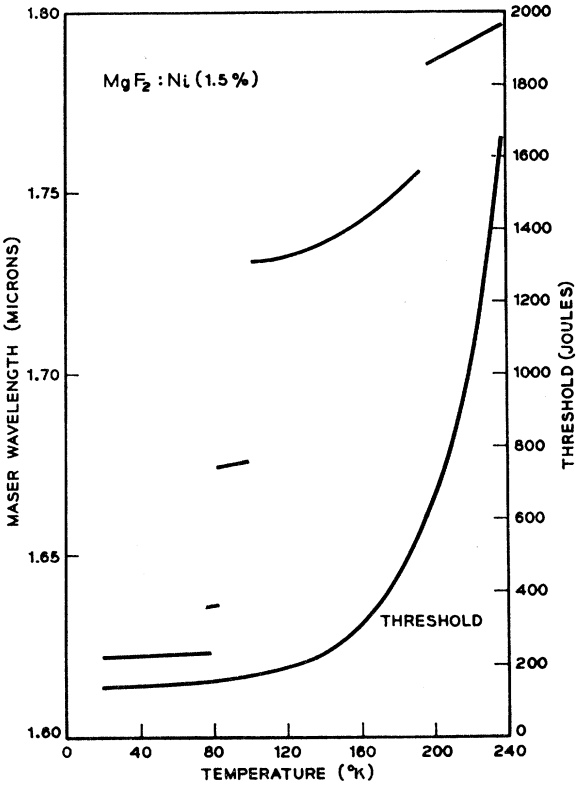

FIG. 4. Temperature dependence of the maser frequency in $MgF_2:Ni^{2+}$ (1.5%). Oscillation occurs in five discontinuous segments between 1.62 and 1.8 μ. The oscillation threshold under pulse illumination in an FT-524 helical xenon lamp is also shown as a function of temperature.

tum efficiency, and concentration. At 81°K the fractional electronic inversion for this crystal at threshold was found to be $N_+/(N_++N_-)=0.006$. N_+ at higher temperatures was scaled according to the threshold

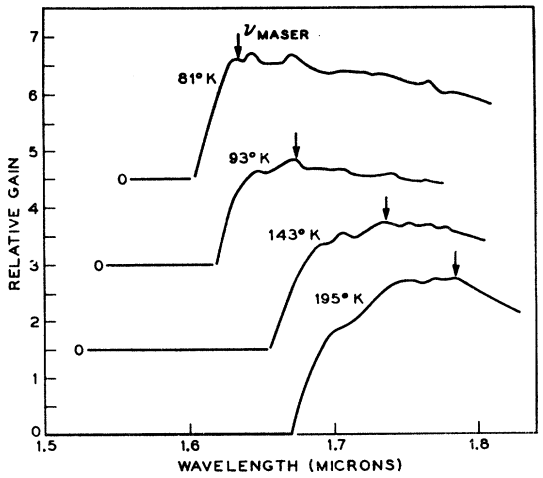

FIG. 5. Gain curves computed from the emission spectra of Fig. 3 and threshold data of Fig. 4. The arrows indicate the maser frequency.

data in Fig. 4. Inspection of Fig. 5 reveals that, except at 81°K, the frequency of maximum gain is in good agreement with the observed maser frequency. The discrepancy at 81°K is attributed to the fact that the frequency of maximum gain at 81°K is very sensitive to N_+.

4. PRISM TUNING

Tunability of $MgF_2:Ni^{2+}$ by means of the wavelength selective feedback provided by an external prism[7,8] has also been demonstrated. A broadband dielectric mirror[9] applied to an 18-in. radius-of-curvature spherical surface of the crystal formed one-half of the resonator; the other end of the crystal was flat and uncoated. A similar dielectric mirror applied to the rear surface of a 35° fused-quartz prism formed the other half of the resonator. The front surface of the prism was oriented at Brewster's angle to the incident light beam and the crystal was cooled by nitrogen gas to about 85°K.

The prism-tuning data, shown in Fig. 6, is somewhat similar to the thermal-tuning behavior of Fig. 4 in that oscillation occurs in the neighborhood of the vibronic maxima. However, since we have not yet been able to tune to frequencies between these maxima, the results obtained thus far by the prism-tuning method have been disappointing. The calculated resolving power appropriate to the illuminated area of the prism is about 50. Yet Fig. 6 indicates considerably poorer wavelength discrimination. We attribute the degradation of resolution to optical distortions within the MgF_2 crystal which produce more or less random angular deviations of the light beam. This, of course, is equivalent to a deterioration in wavelength discrimination within the system. It is apparent from these remarks that successful prism tuning of crystals requires that the utmost attention be paid to the elimination of crystal strain.

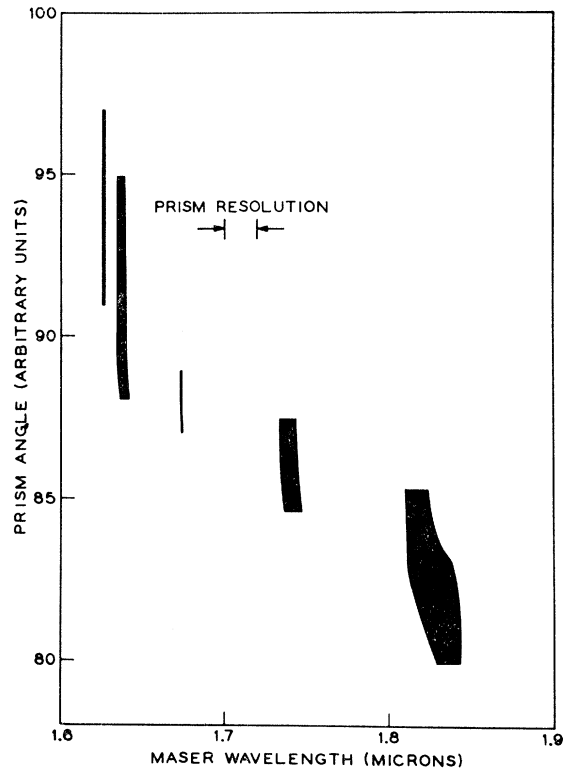

FIG. 6. Prism tuning of coherent emission in $MgF_2:Ni^{2+}$ (1.5%) at 85°K. The horizontal width of the darkened areas indicates the region over which oscillation is observed for a given prism angle.

5. CW OSCILLATION

The broad vibronic sidebands associated with the excited states of Ni^{2+} in MgF_2 are ideal for efficient optical pumping. Furthermore, the fluorescence quantum efficiency is essentially unity when exciting into the low-lying bands in the visible and near infrared (see Fig. 1). The fluorescence lifetime is 3.7, 11.5, and 12.8 msec at 295, 77, and 20°K, respectively. These properties have made it possible to obtain continuous coherent emission at 85°K, requiring less than 65 W of

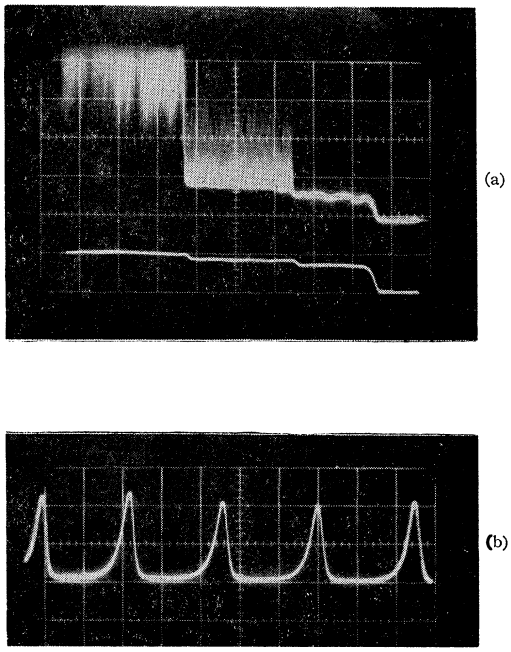

FIG. 7. CW coherent emission from $MgF_2:Ni^{2+}$ at 85°K. (a) The maser output is shown in the upper trace as the power into the tungsten lamp (lower trace) is raised in steps from zero to 155, 175, and 195 W. The time scale is 5 sec per division and increases from right to left. (b) The spiking nature of CW emission close to threshold. The output is essentially zero between the spikes. 1 msec/division.

[7] A. L. Bloom, Appl. Phys. Letters 2, 101 (1963).
[8] A. D. White and J. D. Rigden, Appl. Phys. Letters 2, 211 (1963).
[9] We are indebted to D. L. Perry for applying the dielectric mirrors to the crystals and the prism. The reflectivity of the mirrors was >99.5% over the range 1.51 to 1.99 μ.

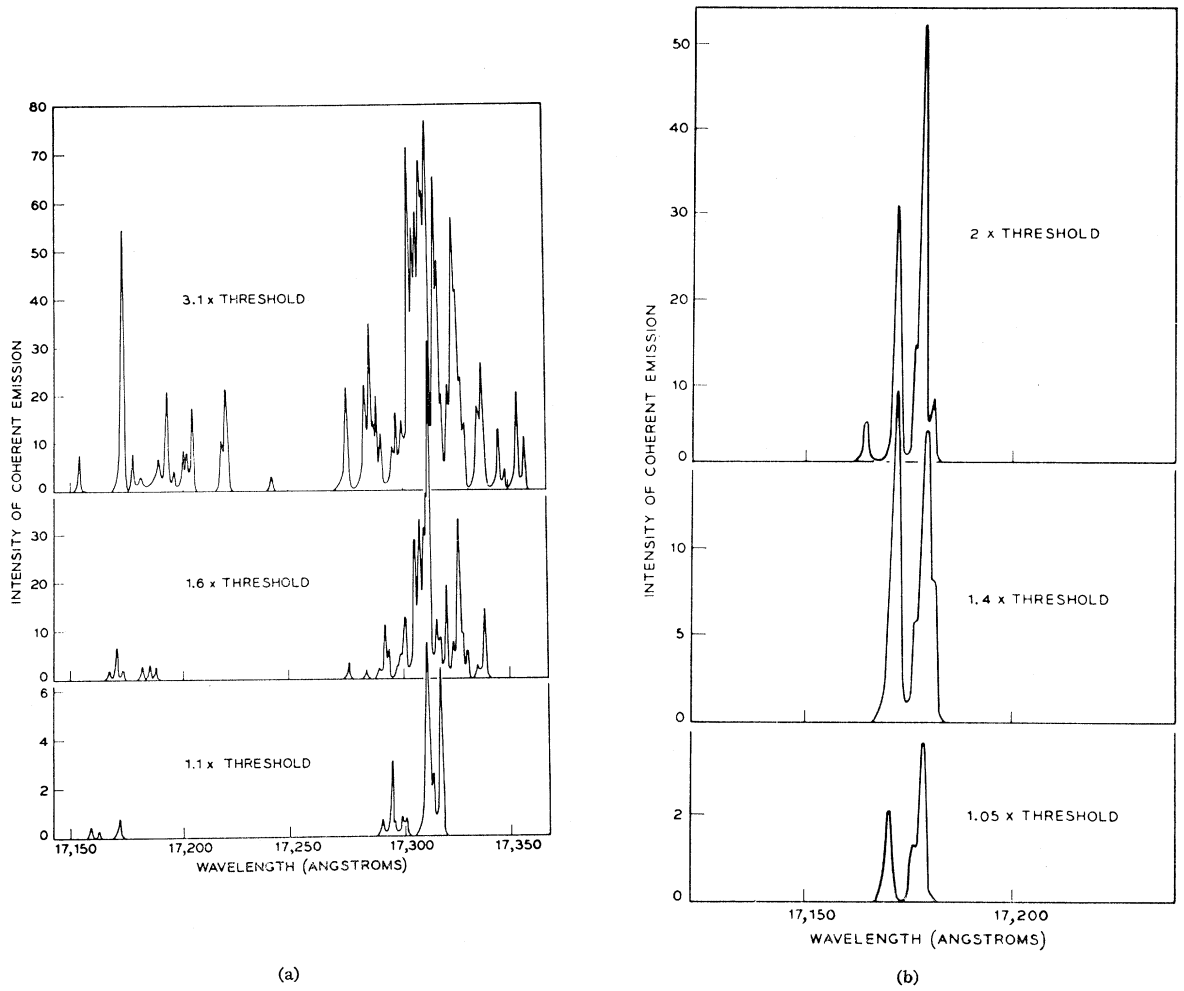

FIG. 8. Dependence of spectral distribution of CW coherent emission on resonator geometry. The apparent width of the various components ($\sim$0.5 cm^{-1}) is instrument limited. (a) Resonator with two spherical mirrors, 7.5 cm radius of curvature. The length of the resonator is 5 cm and the threshold 65 W into a tungsten lamp. (b) Resonator with one flat and one spherical mirror (150-cm radius of curvature). The resonator length is 3 cm and the threshold 190 W.

power into a tungsten lamp. However, a large fraction of the continuous output consists of a train of undamped spikes (Fig. 7). Figure 7(b) shows a pattern consisting of a train of symmetrical spikes each about 300 μsec wide. The interval between spikes decreases with increasing power input. Other crystals have shown spikes with widths as narrow as 20 μsec. We have no satisfactory explanation for this phenomenon at the present time.

The spectral distribution of maser emission can be very complex. Several factors may be responsible: (1) the existence of conditions which permit oscillation in off-axis transverse modes (highly curved mirrors) or which produce off-axis deviations of the beam (crystal strain); (2) the strong temperature dependence of the maser frequency. The effect of mirror curvature is most dramatic and is illustrated by the CW emission spectra shown in Figs. 8(a) and 8(b). One resonator was prepared with highly curved mirrors (7.5 cm radius of curvature), the other with one flat and one spherical mirror of small curvature (150-cm radius). The spectrum for the resonator with highly curved mirrors [Fig. 8(a)] becomes increasingly complex with increasing power input, while the output of the second resonator [Fig. 8(b)] consists essentially of two main components at all input levels. We attribute most, if not all, of the structure present in Fig. 8(a) to oscillation in off-axis transverse modes.[10] Oscillation in a large number of transverse modes is readily sustained in the resonator with highly curved mirrors. These modes are characterized by different threshold populations N_+ and the frequency of maximum gain (the oscillation frequency) for each mode is different, in accordance

[10] G. D. Boyd and J. P. Gordon, Bell System Tech. J. **40**, 489 (1961); A. G. Fox and T. Li, *ibid.* **40**, 453 (1961).

with Eq. (1).[11] On the other hand, the resonator with the flat and the 150-cm radius of curvature mirrors can support only a small number of transverse modes and the spectrum is considerably simpler [Fig. 8(b)].

The effect of crystal strain is somewhat analogous to the effect produced by curved mirrors. Refractive-index variations due to crystal strain produce off-axis deviations of the light beam. These angular deviations constitute variations in threshold across the face of the resonator mirror surfaces. Such a spatial variation in the threshold excited-state population N_+ produces a corresponding spatial variation in the frequency of coherent emission, in accordance with the discussion earlier.

In view of the thermal tunability of $MgF_2:Ni^{2+}$, it is not surprising that temperature gradients influence the spectrum of maser emission. From the thermal tuning data, the temperature coefficient of the maser frequency around 1.73 μ is about 3 Å/°K. A temperature differential of a few degrees within the active volume of the resonator completely smears the structure shown in Fig.. 8(a) and 8(b). For these spectra, gradients were minimized by choosing a resonator diameter no greater than that of the tungsten filament.

A measurement was also made of the CW coherent power output from $MgF_2:Ni^{2+}$ at 85°K. At 500 W into a tungsten lamp, a power output of 1 W was measured with a bolometer. This figure represents an output power averaged over the spikes and not the peak power within the spikes. The mirrors were of very high reflectivity (0.1% transmission) and power conversion efficiencies nearly an order of magnitude greater should be obtained with mirrors optimized for this purpose.

6. DISCUSSION

We have described two methods of tuning the frequency of coherent emission over the vibronic continuum of phonon-terminated optical masers. In addition to thermal tuning and tuning by means of wavelength-selective feedback, it should be pointed out that tuning can also be achieved at fixed temperature without a wavelength-selective element, i.e., with mirrors whose reflectivity is independent of wavelength. This follows from the fact that, if $N_- \exp h(\omega-\omega_0)/kT$ is not negligible compared to N_+ [Eq. (1)], the frequency of highest gain depends on N_+, the upper state population required to reach threshold. As N_+ decreases, the gain curve maximum shifts to lower frequency, where the absorption term is smaller.

Such behavior could be verified experimentally by varying the loss in the resonator (either internal losses or mirror transmission loss). We have not deliberately set out to do this, but the following observation suggests that such behavior does in fact occur. In the early crystals, coherent emission was observed at 77°K at 1.623 μ, i.e., about 340 cm^{-1} from the no-phonon lines.[1] Thresholds were high, i.e., $N_+ \gg N_- \exp[h(\omega-\omega_0)/kT]$ where $h(\omega-\omega_0)=-340$ cm^{-1} and oscillation occurred at the frequency of maximum emission on the vibronic continuum. However, as optical quality improved, the region of oscillation was found to shift to progressively longer wavelengths, occurring first at 1.636 μ rather than at 1.62 μ, then at 1.676 μ instead of either 1.62 or 1.636 μ, and then in the best quality crystals, at 1.717 and 1.733 μ. This is precisely the behavior predicted by McCumber's theory (see Fig. 4 of Ref. 3). From a practical standpoint, it should be remembered that if, for instance, the mirror reflectivity is decreased (e.g. to obtain higher power output), one might also be tuning the maser to a different frequency.

The merits of phonon-terminated optical masers, as exemplified by the low threshold, high efficiency, and tunability of $MgF_2:Ni^{2+}$, must be balanced against the disadvantages of continuous spiking, complex spectral output, and tuning discontinuities. A complex spectral distribution can be avoided with a resonator geometry which prohibits oscillation in transverse modes. The tuning discontinuities hold promise of being eliminated with the hosts MnF_2 and $KMnF_3$. Emission from Ni^{2+} in MnF_2 exhibits what appears to be a perfectly smooth vibronic continuum at 77°K (Fig. 9) and thermal tuning should be free of discontinuities. Tuning of $MnF_2:Ni^{2+}$ by means of an external element will require the elimination of water vapor from the optical path, since the region of oscillation lies in the water band at 1.9 μ. This will not be necessary for $KMnF_3:Ni^{2+}$ since the vibronic continuum is shifted to higher energy.

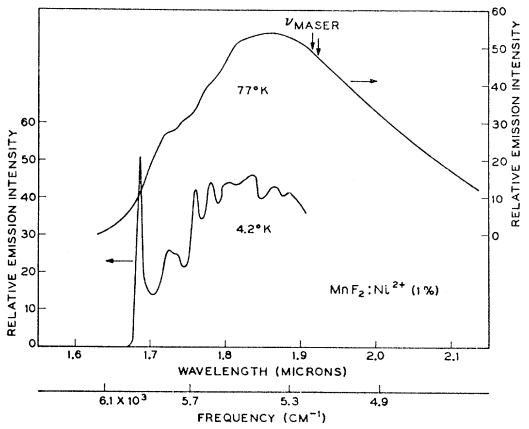

FIG. 9. Fluorescence of Ni^{2+} (1%) in MnF_2 at 4.2 and 77°K, recorded at constant *wavelength* interval. The arrows identify maser frequencies observed at 77°K in two different crystals.

[11] We are not suggesting that the mode separations observed here [Fig. 8(a)] correspond to those given by the Boyd-Gordon theory. The transverse modes defined in the Boyd-Gordon theory must be labeled according to threshold and a gain curve constructed for each mode according to its threshold population N_+. The frequencies corresponding to the maxima of this family of curves are sufficiently different to be observed optically. In effect, the transverse modes have been dispersed in frequency by virtue of their different thresholds.

TABLE I. Summary of characteristics of phonon-terminated optical masers.

Active ion	Host	Temp. (°K)	Maser wavelength (μ)	Transition	Terminal state splitting (cm^{-1})	Lifetime (msec)	Pulse threshold[a] (J)	CW threshold[b] 85°K (W)
Ni^{2+}	MgF_2	77	1.623	$^3T_2 \rightarrow {}^3A_2$	340	11.5	150	
		77–82	1.636		390		160	
		82–100	1.674–1.676		526–533		160–170	240
		100–192	1.731–1.756		723–805		170–570	65
		198–240	1.785–1.797		898–935		570–1650	
	MnF_2	77	1.915	$^3T_2 \rightarrow {}^3A_2$	580[c]	11.1	840	
		20	1.865		560[d]	11.3	740	
		77	1.922		600[c]	11.1	210	
		85	1.929		620[c]			270
		85	1.939		650[c]			240
Ni^{2+}	MgO	77	1.3144	$^3T_2 \rightarrow {}^3A_2$	398		230	
Co^{2+}	MgF_2	77	1.750[e]	$^4T_2 \rightarrow {}^4T_1$	1087	1.3	690	
			1.8035[e]		1256		730	
			1.99		1780		660	
			2.05		1930		700	
	ZnF_2	77	2.165	$^4T_2 \rightarrow {}^4T_1$	1895	0.4	430	
	$KMgF_3$	77	1.821	$^4T_2 \rightarrow {}^4T_1$	1420	3.1	530	
V^{2+}	MgF_2	77	1.1213	$^4T_2 \rightarrow {}^4A_2$	1150	2.3	1070	

[a] The electrical energy into an FT-524 helical xenon lamp.
[b] 500 W T3Q iodine quartz lamp.
[c] Measured from 5800 cm^{-1} (see text).
[d] Measured from 5926 cm^{-1} (see text).
[e] Electronic (no-phonon) lines.

However, oscillation has not yet been obtained in $KMnF_3:Ni^{2+}$.

In Table I we summarize our present information on phonon-terminated optical masers. To avoid too cumbersome a table, only thermal tuning data for $MgF_2:Ni^{2+}$ are given, and that only for one particular crystal. Results vary somewhat with different Ni^{2+} concentration, since both the electronic and vibronic "lines" broaden with increasing concentration. Some of the data on Co^{2+} in MgF_2 and ZnF_2 are taken from Ref. 2. Oscillation from V^{2+} ions in MgF_2 and Co^{2+} in $KMgF_3$ is reported here for the first time.[12] All transitions are phonon-terminated except for two purely electronic transitions in $MgF_2:Co^{2+}$. The maser wavelength refers to the wavelength at the center of a group of oscillating spectral components. In some wavelength regions and for resonators with highly-curved mirrors (see text) the various components may extend over a span of as much as 40 cm^{-1}. Note that oscillation in $MnF_2:Ni^{2+}$ shifts to longer wavelength with decreasing threshold (lower N_+), similar to the behavior described for $MgF_2:Ni^{2+}$.

At 20°K the ground state of Ni^{2+} in MnF_2 is split into three components (at 0, 123, and 255 cm^{-1}) by the exchange field of ordered Mn^{2+} spins[13] and the terminal-state splitting (column 6) is measured from the transition to the lowest component at 5926 cm^{-1}. At 77°K (above the Néel temperature) the ground state is not split by exchange and the terminal-state splitting is measured from the central no-phonon component in the 4°K spectrum at about 5800 cm^{-1} (see Fig. 9).

ACKNOWLEDGMENTS

We express our appreciation to D. L. Perry for preparing dielectric coatings of superb quality and to R. E. Dietz for obtaining the absorption spectrum of $MgF_2:Ni^{2+}$. We are particularly grateful to C. G. B. Garrett and J. K. Galt for advice, ideas, and encouragement throughout the course of this work, and we thank D. E. McCumber for helpful comments on the manuscript.

[12] *Footnote added in proof.* Recently, we have also obtained phonon-terminated coherent emission from Ni^{2+} ions in MgO. The data has been included in Table I.

[13] L. F. Johnson, R. E. Dietz, and H. J. Guggenheim, Phys. Rev. Letters **17**, 13 (1966).

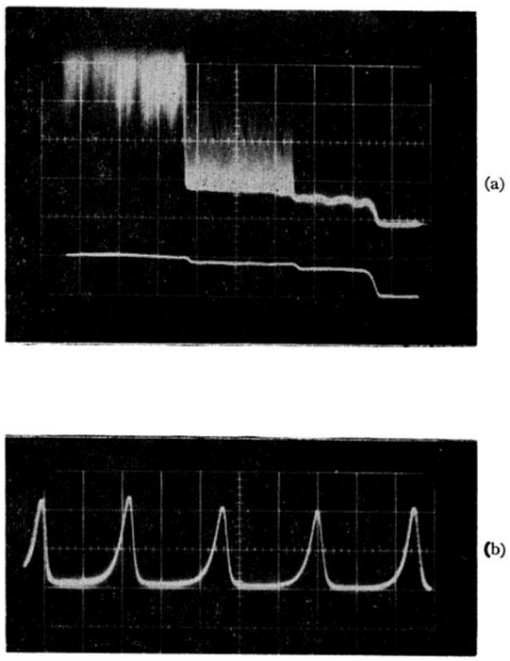

FIG. 7. CW coherent emission from $MgF_2:Ni^{2+}$ at 85°K. (a) The maser output is shown in the upper trace as the power into the tungsten lamp (lower trace) is raised in steps from zero to 155, 175, and 195 W. The time scale is 5 sec per division and increases from right to left. (b) The spiking nature of CW emission close to threshold. The output is essentially zero between the spikes. 1 msec/division.